Study on TAE-Induced Fast-Ion Loss Process in LHD

K. Ogawa, M. Isobe, K. Toi, A. Shimizu, D. A. Spong[1], M. Osakabe, S. Yamamoto[2] and LHD experiment group

National Institute for Fusion Science, Toki, 509-5292, Japan.
[1]Oak Ridge National Laboratory, Oak Ridge, Tennessee, 37831, USA.
[2]Institute for Advanced Energy, Kyoto University, Uji, 611-0011, Japan.
E-mail : ogawa.kunihiro@lhd.nifs.ac.jp

Abstract. Characteristics of fast-ion losses induced by toroidal-Alfvén eigenmode (TAE) have been investigated over wide parameter ranges of the Large Helical Device (LHD) plasmas to reveal the fast-ion loss process. To study fast-ion losses, a scintillator-based lost-fast ion probe (SLIP) is used, and an increment of fast-ion loss flux due to the TAEs from the neoclassical orbit loss level ($\Delta\Gamma_{\text{fast ion}}$) is measured. It is newly found that the dependence of fast-ion loss flux on TAE magnetic fluctuation amplitudes changes at a certain fluctuation level. Experimental results show that in the small TAE magnetic fluctuation amplitude ($b_{\theta\text{TAE}}$) regime, $\Delta\Gamma_{\text{fast ion}}$ is proportional to $b_{\theta\text{TAE}}$ whereas $\Delta\Gamma_{\text{fast ion}}$ increases with the square of $b_{\theta\text{TAE}}$ in the larger $b_{\theta\text{TAE}}$ regime. Simulation by orbit following codes that incorporates magnetic fluctuations with frequency chirping down due to TAEs suggests the change of the fast-ion loss process from a convective ($\Delta\Gamma_{\text{fast ion}} \propto b_{\theta\text{TAE}}$) to a diffusive ($\Delta\Gamma_{\text{fast ion}} \propto b_{\theta\text{TAE}}^2$) character as $b_{\theta\text{TAE}}$ increases.

PACS : 52.35.Bj, 52.25.Gj, 52.55.Pi, 52.55.Hc, 52.25.Fi

1. Introduction

One of the critical issues in realizing self-sustained DT burning plasma is that how well alpha particles will be confined, since alpha particles are a primary heat source in the plasma. During the slowing down of alpha particles due to Coulomb collisions, the alpha particles can excite the fast-ion-driven magnetohydrodynamic (MHD) modes such as toroidal-Alfvén eigenmode (TAE) which are predicted to induce a localized damage on plasma facing components due to the impact of alpha particle losses. Better understanding of transport and loss processes of alpha particles is required to reduce the alpha particles losses for avoidance of the problem. After the first experiment to excite TAEs in TFTR [1], a large number of studies have been conducted to understand the effect of TAEs on fast-ion transports and/or losses in tokamaks. Considerable progress in understanding on TAE physics has been

achieved and the knowledge will be applied to an ITER plasma [2]. TAE research had also been performed in heliotron/stellarator devices [3] such as compact helical system (CHS) [4] and Wendelstein 7-AS [5]. These devices have two differences from the tokamaks: a non-axisymmetric magnetic field configuration and a different safety factor profile. So, comparison studies in tokamaks and heliotron/stellarator devices are very beneficial for clarifying the interaction between fast ions and TAEs in magnetically confined toroidal plasmas. The first observation of TAE in heliotron/stellarator devices was achieved in CHS [6]. The TAE profile measured by a soft-x-ray array and a heavy ion beam probe is consistent with TAE structure predicted by CAS3D3 code [4]. After that, fast-ion losses due to TAE having relatively large amplitude were measured by scintillator-based lost-fast ion probe (SLIP) [7]. They concluded that the fast ion loss flux would be sensitively dependent on the internal structure of the eigenmode as well as the mode amplitude levels. In the Large Helical Device (LHD), radial transport and loss of fast ions due to TAEs and energetic-particle modes have been observed using a neutral particle analyzer and a SLIP [8-10]. Experiments have shown that fast-ion loss rate increases as TAE magnetic fluctuation amplitude ($b_{\theta TAE}$) increases as expected. Experiments have indicated that the process of fast-ion loss caused by TAEs changes from convective type to diffusive type, and vice versa according to magnetic configurations. It is associated with the radial extent of the TAE eigenfunction and fast-ion orbit width [11]. Recently, we have found that in addition to magnetic configuration, the process of fast-ion loss also changes according to $b_{\theta TAE}$ even in fixed configuration. Previous theoretical modeling for axisymmetric tokamak predicts that the process of TAE-induced fast-ion transport changes from a convective type to a diffusive type as $b_{\theta TAE}$ increases [12]. In this paper, we report experimentally observed characteristics of fast-ion loss caused by TAE in non-axisymmetric system. We also make a comparison between experiment and simulation with the aid of orbit-following particle calculation that incorporates TAE magnetic fluctuations.

2. Experimental setups

LHD shown in Fig. 1 is the largest heliotron device in the world having a major radius of 3.90 m and an average plasma minor radius (a) of ~0.6 m. In experiments described in this paper, a direction of the toroidal magnetic field (Bt) is in the counter clock wise from the top view. In this case, one of neutral beam injector (NB2) injects neutral beams in the counter direction while NB1 and NB3 inject beams in the co-direction. Fast ions created by these beams with injection energy up to 180 keV are super Alfvénic in this experiment. Fast-ion loss is measured by a SLIP. This instrument is essentially a magnetic spectrometer using LHD magnetic field, consisting of a pair of apertures and a scintillator plate. Bright spots on the scintillator due to impact of fast ions give information of the energy (E) and pitch angle

(χ=arccos($v_{//}/v$)) of those ions, simultaneously. Here, v and $v_{//}$ stand for the velocity of the ions and its parallel component to the magnetic field line, respectively. The SLIP installed on the LHD is designed so as to detect the fast ions having the E of 2 keV to 400 keV at Bt=0.6 T and χ of 20 to 70 degrees. Scintillation lights due to the impact of fast ions are measured using 16 photomultipliers (PMTs). Each PMT views particular region of E and χ of the screen. The system time response is, about 200 kHz, high enough to observe rapid phenomena such as TAE-induced fast-ion loss. Detailed structure and function of the SLIP are described in Refs. 13 and 14. The poloidal magnetic fluctuation amplitude of TAE ($b_{\theta TAE}$) is measured by a Mirnov coil placed on the vacuum vessel. Toroidal mode number (n) and poloidal mode number (m) of TAE are identified by Mirnov coils arrays. The electron temperature (T_e) and the electron density (n_e) profiles are provided by Thomson scattering diagnostics [15]. The line-averaged density ($<n_e>$) is measured with a multi-channel far-infrared laser interferometer [16].

3. Experimental results

Measurements of fast-ion losses induced by TAE instabilities are performed in NB-heated LHD plasmas having three magnetic axis positions at finite beta, i.e. R_{mag}=3.75m (case A), 3.86 m (case B), and 4.00 m (case C). As R_{mag} becomes larger, fast-ion orbits tend to deviate largely from magnetic flux surfaces as shown in Fig. 2 (a). Note that the TAE gap becomes wider with larger R_{mag} compared with smaller R_{mag} since magnetic shear in LHD becomes weaker as R_{mag} becomes larger as shown in Fig. 2 (b). The typical wave forms of NB power absorbed by the plasma (P_{NB}), the electron temperature at the magnetic axis (T_{e0}), the volume-averaged plasma beta ($<\beta>$),$<n_e>$, and the magnetic fluctuation spectrogram in case B are shown in Fig. 3. As shown in Fig. 3, the strong magnetic fluctuation appears in the frequencies of ~70 kHz. Also low frequency fluctuation less than 10 kHz is recognized. The Mirnov array reveals that the higher frequency mode has a structure of m/n=~1/1 TAE. The lower frequency mode is recognized as resistive interchange mode excited by steep gradient of the bulk plasma pressure at edge region [18].

Enhancement of fast-ion loss flux due to TAE is observed in the region of E of 50-180 keV and χ of 35-45 degrees using the SLIP. Note that fast-ion loss correlated with resistive interchange mode is seen on entire region of E and χ [9]. In this paper, to focus on the behavior of fast-ion loss due to TAEs, the effect of a resistive interchange mode on a fast-ion loss is removed using a numerical band-stop filter in the frequency range from 0.8 kHz to 1.2 kHz. Time traces of magnetic fluctuations on the TAE frequency range and the fast-ion loss flux ($\Gamma_{fast\ ion}$) in case B are shown in Fig. 4. Increases of $\Gamma_{fast\ ion}$ correlate with recurrent bursts of TAE are seen. Figure 5 shows the dependence of $\Delta\Gamma_{fast\ ion}$ normalized by fast-ion populations created by co-injected NB, i.e. $P_{NBco}\times\tau_s$ on $b_{\theta TAE}/Bt$ in cases A, B, and C. Here,

$\Delta\Gamma_{\text{fast ion}}$, P_{NBco} and τ_s stand for increments of fast-ion loss flux due to TAEs from the neoclassical orbit loss level, the absorbed power of co-injected NBs and the Spitzer slowing down time, respectively. As shown in Fig. 5, the dependence of $\Delta\Gamma_{\text{fast ion}}/(P_{\text{NBco}}\times\tau_s)$ on $b_{\theta\text{TAE}}/Bt$ is changed at $b_{\theta\text{TAE}}/Bt \sim 7\times10^{-5}$ in case B. In a small $b_{\theta\text{TAE}}$ regime, $\Delta\Gamma_{\text{fast ion}}/(P_{\text{NBco}}\times\tau_s)$ is proportional to $b_{\theta\text{TAE}}/Bt$ whereas in a large $b_{\theta\text{TAE}}$ regime, $\Delta\Gamma_{\text{fast ion}}/(P_{\text{NBco}}\times\tau_s)$ increases with the square of $b_{\theta\text{TAE}}/Bt$. In case A, $\Delta\Gamma_{\text{fast ion}}/(P_{\text{NBco}}\times\tau_s)$ is proportional to $b_{\theta\text{TAE}}/Bt$ in a small $b_{\theta\text{TAE}}/Bt$ region. In case C, $\Delta\Gamma_{\text{fast ion}}/(P_{\text{NBco}}\times\tau_s)$ is proportional to $(b_{\theta\text{TAE}}/Bt)^3$. The change of dependence of fast-ion loss flux on magnetic fluctuation amplitude has not been observed for these $b_{\theta\text{TAE}}/Bt$ ranges although the change may appear in unexplored regions in cases A and C.

4. Orbit following models including TAE fluctuation

A numerical simulation based on orbit following models including TAE fluctuation is performed to study the change of dependence of the fast-ion loss flux on TAE magnetic fluctuation amplitude observed in experiment. Calculation scheme is as follows. The three dimensional MHD equilibrium is reconstructed by VMEC2000 code [19] in the fixed-boundary condition. Next, the birth profile of fast ions created by NB injection is calculated by the HFREYA code [20]. Finally, the guiding-center orbit of each fast ion is followed using the DELTA5D code [21] that includes time-varying TAE fluctuation of which structure is given from the eigenfunction calculated by AE3D code. Velocity distribution function of fast ion created by NB injection is formed by the method written in Ref. 11. The Coulomb collisions between fast ions and the bulk plasma are taken into account. This simulation is applicable to a confined plasma region inside of LCFS, because they are based on the VMEC equilibrium. In the vacuum region outside the LCFS, Lorentz orbit code is used as explained later. Because TAE is classified into the shear Alfvén type which is mainly composed of perpendicular components to magnetic field lines, TAE fluctuation is modeled as $\boldsymbol{b}=\nabla\times(\alpha\boldsymbol{B})$. Here, α represents a general function of the position, frequency, and amplitude of the magnetic fluctuation. Radial structure of α is given based on the eigenfunction of TAE calculated by AE3D as shown in Fig. 2 (b). The TAEs have a mode structure of m/n=1+2/1 and are characterized by a relatively wide radial profile. Note that profile of n_e fluctuation due to TAE evaluated from AE3D eigenfunction agree well with that measured in experiments [9]. Frequency of α is set to be the same as the TAE frequency measured in experiments. Frequency chirping down rate is assumed to be 20 kHz/ms as seen in experimentally observed TAE burst. Amplitude of α is obtained from the TAE fluctuation amplitude measured by Mirnov coil. According to Ref. 11, $b_{\theta\text{TAE}}$ is expressed as $b_{\theta\text{TAE}}\sim\alpha_0\times b_{\theta\text{TAE LCFS}}/b_{\theta\text{TAE peak}}(r_{\text{Mirnov}}/a)^{-(m+1)}(r_v^{2m}+r_{\text{Mirnov}}^{2m})(r_v^{2m}+a^{2m})^{-1}$. Here, α_0, r_{Mirnov}, r_v, $b_{\theta\text{TAE LCFS}}$, and $b_{\theta\text{TAE peak}}$ stand for peak amplitude of α, radial position of Mirnov coil, radial position of vacuum vessel, the calculated poloidal magnetic fluctuation amplitude at LCFS, and that at TAE peak,

respectively. The amplitude of α is obtained from the above equation. In this code, the effect of the potential produced by electrons eliminating the electric field parallel to the magnetic field is included. Because of this, fast-ion motion is further modified by the fact that the rapid mobility of the electrons makes the electric field experienced by the ions parallel to the magnetic field equal to zero. Because DELTA5D is applicable only to the fast-ion orbit inside the LCFS, we use Lorentz orbit code to follow the orbit outside of the LCFS. It is also necessary to calculate fast-ion orbits reaching the SLIP since it works as a magnetic spectrometer.

5. Results of the orbit simulation

Figure 6 shows calculated $\Delta\Gamma_{\text{fast ion}}/(P_{\text{NBco}}\times\tau_s)$ as a function of $b_{\theta\text{TAE}}/Bt$ for cases A and B. In case B, as observed in experiment (see Fig. 5), the change of fast-ion loss flux dependence on the magnetic fluctuation amplitude is obtained in the simulation. In the small $b_{\theta\text{TAE}}$ regime, $\Delta\Gamma_{\text{fast ion}}/(P_{\text{NBco}}\times\tau_s)$ is proportional to $b_{\theta\text{TAE}}/Bt$ whereas $\Delta\Gamma_{\text{fast ion}}/(P_{\text{NBco}}\times\tau_s)$ increases with the square of $b_{\theta\text{TAE}}/Bt$ in a large $b_{\theta\text{TAE}}$ regime. The critical value of $b_{\theta\text{TAE}}/Bt$ is $\sim 3\times10^{-5}$ which is the same order of that in experiments $\sim 7\times10^{-5}$. According to theory by Sigmar [12], $\Delta\Gamma_{\text{fast ion}}$ proportional to $b_{\theta\text{TAE}}$ is suggested to be due to a convective type loss process whereas $\Delta\Gamma_{\text{fast ion}}$ scaling as the square of $b_{\theta\text{TAE}}$ is suggested to be due to a diffusive type loss process. The simulation and experimental results indicate that the fast-ion loss process changes from convective to diffusive in case B. Also in case A, as observed in experiment, $\Delta\Gamma_{\text{fast ion}}/(P_{\text{NBco}}\times\tau_s)$ increases linearly with $b_{\theta\text{TAE}}/Bt$ in small $b_{\theta\text{TAE}}/Bt$ regime and tends to saturate as $b_{\theta\text{TAE}}/Bt$ increases. It is interesting to note that saturation of $\Delta\Gamma_{\text{fast ion}}/(P_{\text{NBco}}\times\tau_s)$ is seen at $b_{\theta\text{TAE}}/Bt$ from $\sim 2\times10^{-5}$ to $\sim 1\times10^{-4}$. The change of the loss dependence appears when $b_{\theta\text{TAE}}/Bt$ goes up further. The loss dependence becomes a quadratic character at $b_{\theta\text{TAE}}/Bt$ of $\sim 10^{-4}$ that is in unexplored regions of experiments. Note that E and χ regions of fast ions reaching to the SLIP are 120-180 keV and of 30-40 degrees, respectively. These are similar to the experimentally measured E and χ.

The orbit simulation shows the detail of the fast-ion loss process due to TAE. Figure 7 shows the number of lost-fast ions as a function of their birth positions in case A. The lost-fast ions increase with the increase of $b_{\theta\text{TAE}}/Bt$ as expected. On the calculation without TAE, there are two peaks which correspond to the inner side and the outer side of orbits of fast ions escaping from the plasma, respectively. Note that the asymmetry of the profile is due to the deviation of co-going fast-ion orbits from the flux surface as seen in Fig. 2 (a). In the small $b_{\theta\text{TAE}}/Bt$ cases i.e. $b_{\theta\text{TAE}}/Bt$ of 1×10^{-5} and 6×10^{-5}, losses of fast ions deposited near the confinement/loss boundary increase whereas losses of fast ions deposited on interior region noticeably increase in large $b_{\theta\text{TAE}}/Bt$ cases i.e. $b_{\theta\text{TAE}}/Bt$ of 2×10^{-4}. Figure 7 suggests that the saturation of $\Delta\Gamma_{\text{fast ion}}/(P_{\text{NBco}}\times\tau_s)$ appears because not enough fast ions left near the confinement/loss boundary.

To make the transport process visible, orbits of barely confined fast ions near the confinement/loss boundary and fast ions confined interior region are shown in Figs. 8 and 9, respectively. As seen in Fig. 8 (b), barely confined fast ions near the confinement/loss boundary escape from the plasma due to the radial excursion by TAE fluctuation immediately in small $b_{\theta TAE}$ case. Because the radial excursion increases lineally with $b_{\theta TAE}$, the fast ion into the loss region is proportional to $b_{\theta TAE}$, i.e. the fast-ion loss flux having this type of orbit is proportional to $b_{\theta TAE}$. As mentioned before, fast-ion loss having this dependence on $b_{\theta TAE}$ is referred as convective loss. It can be therefore reasonably concluded that experimentally observed fast-ion loss due to small $b_{\theta TAE}$ is caused dominantly by a convective transport. Orbits of fast ions confined interior region tend to expand toward the outboard side of the torus as the TAE amplitude increase as seen in Fig. 9. As shown in Fig. 9 (b), as has been suggested, the fast ion does not escape from the plasma in small $b_{\theta TAE}$ case. In large $b_{\theta TAE}$ case, orbit of a fast ion expands gradually, then finally, the fast ion is lost from the confinement domain as shown in Fig. 9 (c). The displacement of fast-ion orbits due to mode overlapping leads to the transient growth of the broadening of the fast-ion spatial distribution. Because the growth of the broadening scales as $b_{\theta TAE}^2$, flux of fast ions escaping from the plasma is expected to be proportional to $b_{\theta TAE}^2$, and this is diffusive loss as mentioned before. It can be concluded, from what has mentioned above, that experimentally observed fast-ion loss due to large $b_{\theta TAE}$ is caused dominantly by a diffusive transport.

6. Summary

Characteristics of fast-ion loss process due to TAE are studied in LHD plasmas using the SLIP. It is found that in the smaller $b_{\theta TAE}$ regime, $\Delta\Gamma_{\text{fast ion}}$ is proportional to $b_{\theta TAE}$, whereas in large $b_{\theta TAE}$ regime, $\Delta\Gamma_{\text{fast ion}}$ increases with the square of $b_{\theta TAE}$. To understand the change of the dependence in three dimensional LHD plasma precisely, simulations based on an orbit following models that incorporates TAE magnetic fluctuations with frequency chirping down and radial profile of TAE are performed. The simulation reproduces the change of the loss process from convective ($\Delta\Gamma_{\text{fast ion}} \propto b_{\theta TAE}$) to diffusive ($\Delta\Gamma_{\text{fast ion}} \propto b_{\theta TAE}^2$) according to magnetic fluctuation amplitude. Orbit simulation shows that with a convective type loss process, the barely confined fast ion near the confinement/loss boundary is lost due to TAE with small amplitude whereas the fast ion confined in the interior region of the plasma is lost with a diffusive type loss process due to TAE with large amplitude. In small $b_{\theta TAE}$ region, convective type loss is thought to be dominant. As $b_{\theta TAE}$ increases, diffusive type loss increases and exceeds the convective type loss at a certain $b_{\theta TAE}$ level. The change of fast-ion loss process observed in experiments is explained by the change of the dominant loss process.

Acknowledgements

This work was supported in part by the Grant-in-Aid for Scientific Research from JSPS Nos. 21360457, 21340175 and 22-7912, from the LHD project budget (NIFS12ULHH003), and Japan/U.S. Cooperation in Fusion Research and Development. The authors are grateful to the LHD operation group for their excellent technical support.

References

[1] K. McGuire, R. Goldston, M. Bell *et al*., 1983 Phys. Rev. Lett. **50** 891.
[2] A. Fasoli, C. Gormenzano, H. L. Berk *et al*., 2007 Nucl. Fusion **47** S264.
[3] K. Toi, K. Ogawa, M. Isobe *et al*., 2011 Plasma Phys. Control. Fusion **53** 024008.
[4] K. Toi, M. Takechi, M. Isobe *et al*., 2000 Nucl. Fusion **40** 1349.
[5] A. Weller, M. Anton, J. Geiger *et al*., 2001 Phys. Plasmas **8** 931.
[6] M. Takechi, K. Toi, S. Takagi *et al*., 1999 Phys. Rev. Lett. **83** 312.
[7] M. Isobe, K. Toi, H. Matsushita *et al*., 2006 Nucl. Fusion **46** S918.
[8] M. Osakabe, S. Yamamoto, K. Toi *et al*., 2006 Nucl. Fusion **46** S911.
[9] K. Ogawa, M. Isobe, K. Toi *et al*., 2010 Nucl. Fusion **50** 084005.
[10] M. Isobe, K. Ogawa, K. Toi, *et al*., 2010 Contrib. Plasma Phys. **50** 540.
[11] K. Ogawa, M. Isobe, K. Toi *et al*., 2012 Nucl Fusion **52** 094013.
[12] D. J. Sigmar, C. T. Hsu, R. B. White *et al*., 1992 Phys. Fluids B **4** 6.
[13] K. Ogawa, M. Isobe and K. Toi, 2009 J. Plasma Fusion Res. Series **8** 655.
[14] K. Ogawa, M. Isobe and K. Toi, 2008 Plasma Fusion Res. **3** S1082.
[15] I. Yamada, K. Narihara, H. Funaba *et al*., 2010 Fusion Sci. Tech. **58** 345.
[16] T. Akiyama, K. Kawahata, K. Tanaka *et al*., 2010 Fusion Sci. Tech. **58** 352.
[17] D. A. Spong, E. D'azevedo and Y. Todo, 2010 Phys. Plasmas **17** 022106.
[18] F. Watanabe, K. Toi, S. Ohdachi *et al*., 2007 Plasma Fusion Res. **2** S1066.
[19] S. P. Hirshman and O. Betancourt, 1991 J. Comput. Phys. **96** 99.
[20] S. Murakami, N. Nakajima, M. Okamoto *et al*., 1995 Trans. Fusion Technol. **27** 256.
[21] D. A. Spong , 2011 Phys. Plasmas **18**, 056109.

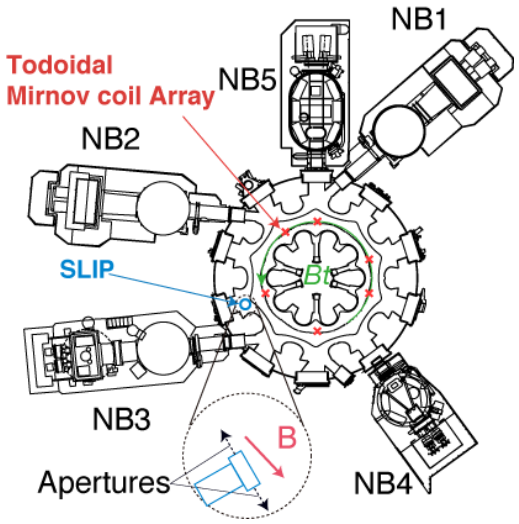

Fig. 1 Top view of the LHD, NB injectors, the SLIP, and the positions of Mirnov coils.

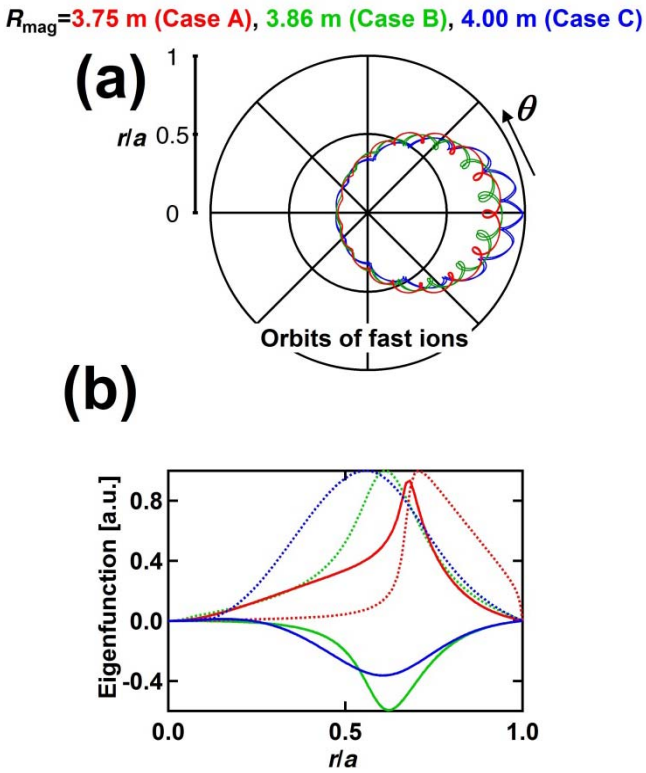

Fig. 2 (a) Poloidal projection of co-circulating fast-ion orbits in cases A (R_{mag}=3.75 m), B (R_{mag}=3.86 m), and C (R_{mag}=4.00 m) on Bt= 0.6 T. E and χ of fast ions are 180 keV and 30 degrees, respectively. The deviation of orbits from the flux surface increases as the increase of R_{mag}. (b) Eigenfunctions of TAE calculated by AE3D [17] for cases A, B, and C.

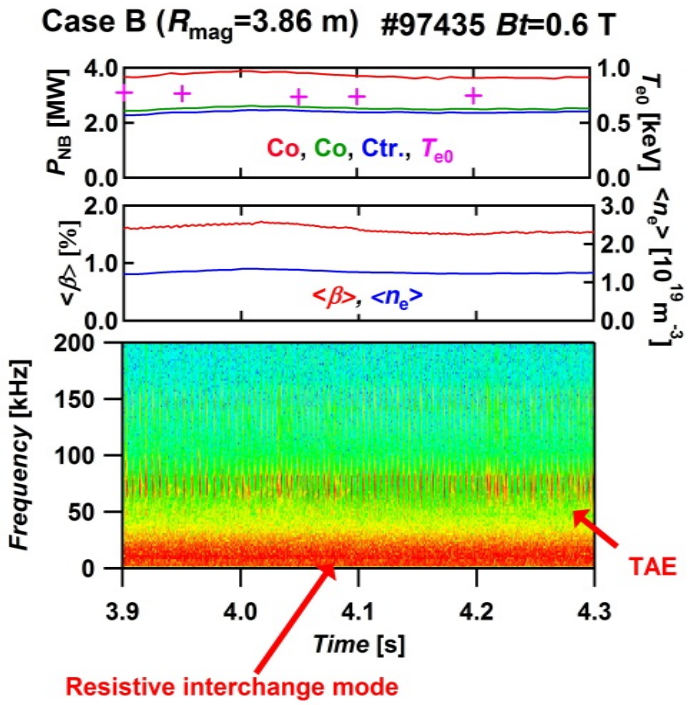

Fig. 3 Typical wave forms of TAE excitation experiments. The perturbation whose frequency is ~70 kHz is identified as TAE from the magnetic fluctuation analysis. Another perturbation whose frequency is < 10 kHz is recognized as resistive interchange mode excited at the plasma edge region. No significant change of plasma parameters is observed on this time range.

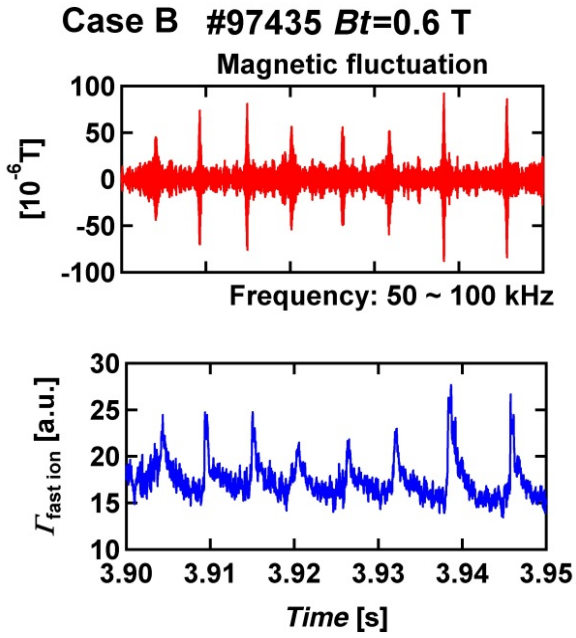

Fig. 4 Time traces of magnetic fluctuation for TAE range of frequency and $\Gamma_{\text{fast ion}}$ on the condition of Bt = 0.6 T. Small and large increases of $\Gamma_{\text{fast ion}}$ due to small and large TAEs are observed, respectively.

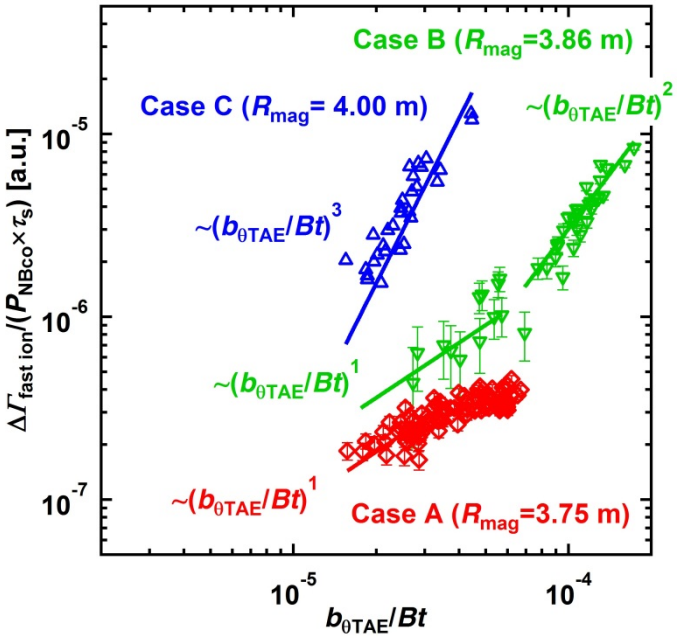

Fig 5 $\Delta\Gamma_{fast\ ion}/(P_{NBco}\times\tau_s)$ as a function of $b_{\theta TAE}/Bt$ in cases A, B and C. Dependence of fast-ion loss flux on $b_{\theta TAE}/Bt$ changes at $b_{\theta TAE}/Bt\sim7\times10^{-5}$ in case B.

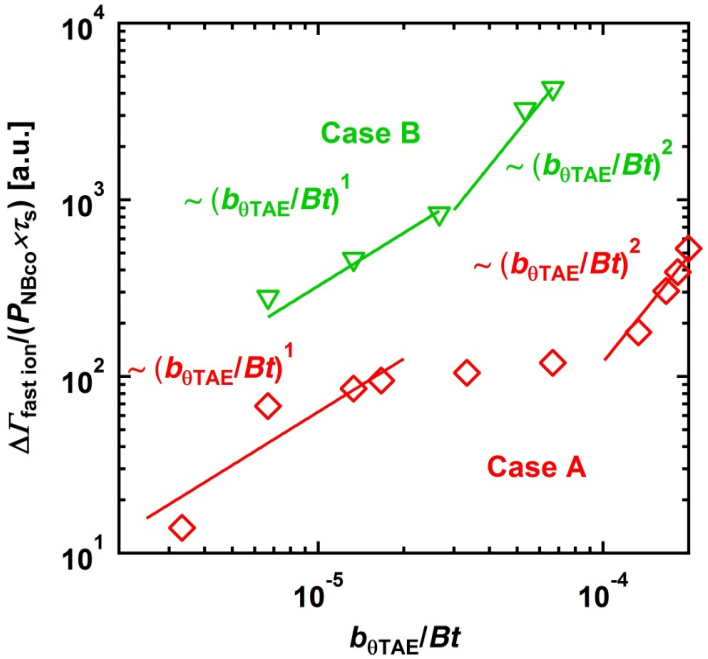

Fig 6 $\Delta\Gamma_{fast\ ion}/(P_{NBco}\times\tau_s)$ as a function of $b_{\theta TAE}/Bt$ in calculations for cases A and B. The dependence is similar to that obtained in experiments in case A in the small $b_{\theta TAE}$ regime. The change of the loss process from a convective type to a diffusive type is reproduced by simulation for case B.

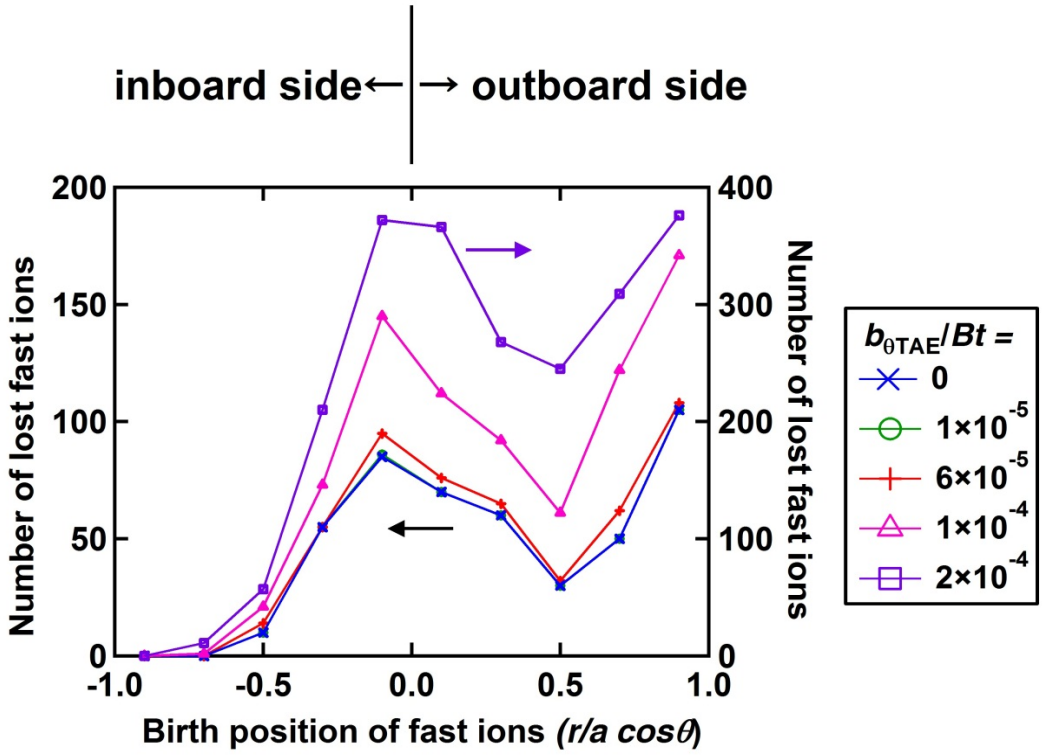

Fig. 7 Number of lost-fast ions as a function of their birth position in case A.

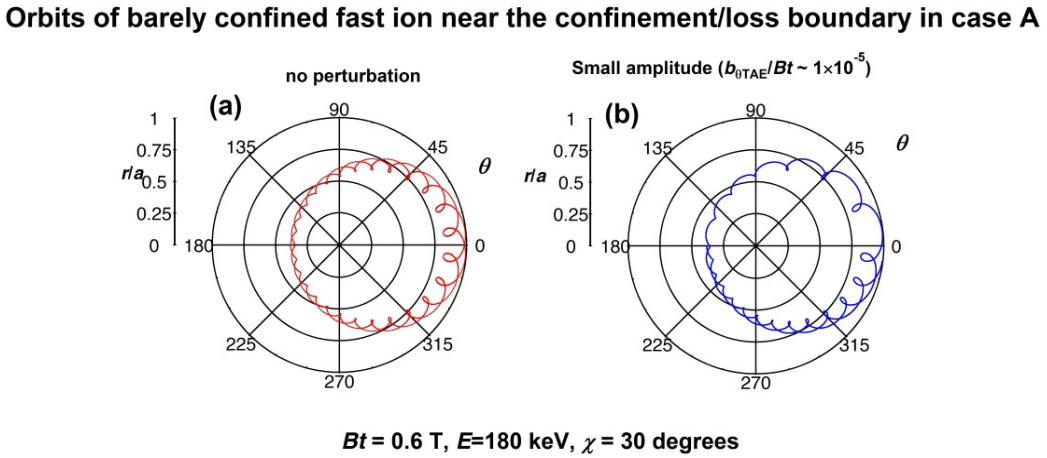

Fig. 8 Orbits of barely confined fast ions near the confinement/loss boundary without TAE (a) and with small TAE (b) in case A. The fast ion is lost with small TAE with convective process.

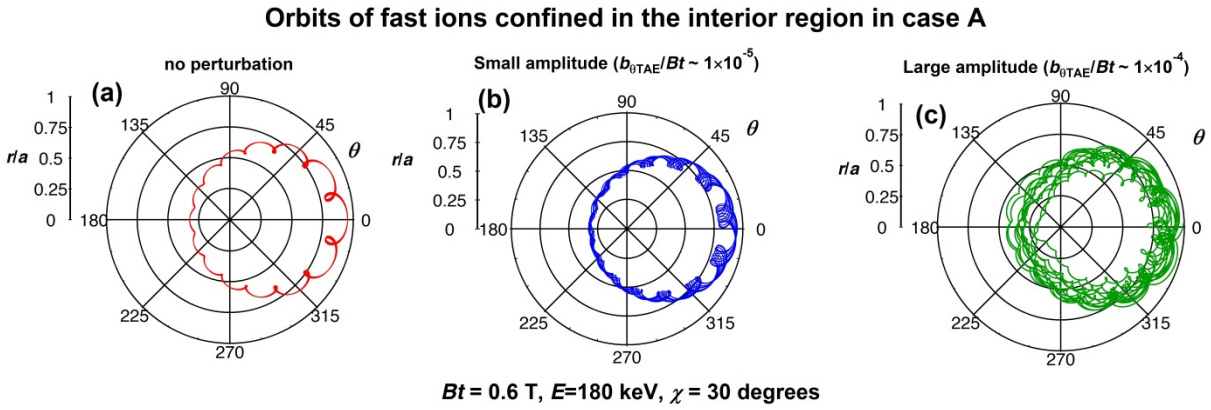

Fig. 9 Orbits of fast ions existing interior region without TAE (a), with small TAE (b), and with large TAE (c) in case A. The TAE fluctuation affects the fast-ion orbit repeatedly. The fast ion is lost with large TAE with diffusive process.